Available online at www.sciencedirect.com
SCIENCE DIRECT
Journal of Power Sources 153 (2006) 274–280
JOURNAL OF POWER SOURCES
www.elsevier.com/locate/jpowsour

Porous olivine composites synthesized by sol–gel technique

R. Dominko [a,*], M. Bele [a], M. Gaberscek [a], M. Remskar [b], D. Hanzel [b], J.M. Goupil [c], S. Pejovnik [d], J. Jamnik [a]

[a] *National Institute of Chemistry, P.O. Box 660, SI-1001 Ljubljana, Slovenia*
[b] *Jozef Stefan Institute, Jamova 39, SI-1000 Ljubljana, Slovenia*
[c] *ENSICAEN, UMR CNRS 6506, Catalyse & Spectrochimie Lab, F-14050 Caen, France*
[d] *Faculty of Chemistry and Chemical Technology, University of Ljubljana, Aškerčeva 5, SI-1000 Ljubljana, Slovenia*

Available online 29 June 2005

Abstract

Porous $LiMPO_4$/C composites (where M stands for Fe and/or Mn) with micro-sized particles were synthesised by sol–gel technique. Particles porosity is discussed in terms of qualitative results obtained from SEM micrographs and in terms of quantitative results obtained from N_2 adsorption isotherms. Porous particles could be described as an inverse picture of nanoparticulate arrangement, where the pores serve as channels for lithium supply and the distance between the pores determines the materials kinetics. Tests show that the electrochemical behaviour of porous $LiMPO_4$/C composite is comparable with the results from the literature. The best electrochemical results were obtained with a $LiFePO_4$/C composite (over 140 mAh g^{-1} at *C*/2 rate during continuous cycling). The capacity obtained with $LiMnPO_4$/C composite is much lower (40 mAh g^{-1} at *C*/20 rate), although the textural properties are similar to those observed in the $LiFePO_4$/C composite.

Keywords: Porous composites; Cathode material; $LiMPO_4$; Sol–gel synthesis; Citric acid; Li-ion batteries

1. Introduction

Since the pioneering work of Goodenough and co-workers [1], the phospho-olivines $LiMPO_4$ (where M stands for Fe, Mn, Co, Ni) have been recognized as a potential positive electrode material for use in lithium ion batteries. Although this family of materials posses a number of advantages (high capacity, stability during lithium extraction/insertion), their main drawback is poor electrochemical performance due to sluggish kinetics. Besides their high capacity (close to 170 mAh g^{-1}), $LiMPO_4$ cathode materials show high stability during lithium extraction/insertion and do not deteriorate when used at moderately high temperatures. Recently, a lot of efforts have been devoted to optimization of $LiFePO_4$ material [2,3]. Surprisingly, only a few papers indicate the applicability of $LiMnPO_4$ [4–7] and, besides that, the results remain controversial. The origin of the different electrochemical activities of isostructural $LiFePO_4$ and $LiMnPO_4$ is not quite clear at the moment. Yamada and Chung [4] suggested that the low electrochemical activity of $LiMnPO_4$ was due to slow kinetics and internal friction during lithium extraction/insertion. In our recent work a comparative structural study [8] of these two materials showed minute differences in the oxygen vibrations in the Li layer. Comparing magnetic ground state of $LiMPO_4$ (M = Fe or/and Mn) we have found [9] that $LiMnPO_4$ is very sensitive to various crystal imperfections and readily changes from the collinear antiferromagnetic state to a week ferromagnetic state, while $LiFePO_4$ collinear antiferromagntic state is very robust.

In the literature, a common opinion is that the $LiFePO_4$ material has to be in nanoparticulate form with intimate carbon contact [2,3,10–12] or doped with a supervalent metal ion [13] at Li^+ site in order to achieve full capacity at room temperature, regardless of the type of synthesis. In our recent work [14] we have shown that with careful selection of starting precursors, preparation of $LiFePO_4$ compounds leads to porous micro-sized particles, which give comparable electrochemical characteristics as those in nanoparticulate form. Namely, in a porous material the pore-to-pore distance deter-

* Corresponding author. Tel.: +386 14760319; fax: +386 14760300.
E-mail address: Robert.Dominko@ki.si (R. Dominko).

0378-7753/$ – see front matter © 2005 Elsevier B.V. All rights reserved.
doi:10.1016/j.jpowsour.2005.05.033

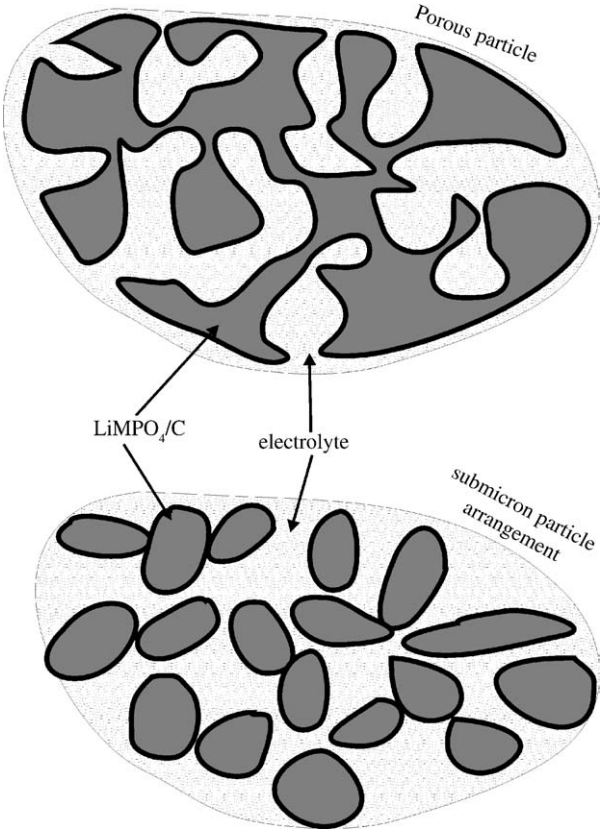

Fig. 1. Shematic presentation of (a) porous system and (b) submicron particles arangment.

mines the solid-state diffusion of lithium. Apparently, this distance has a similar value as the average diameter of nanoparticles in particulate materials. Differences between the porous structure and sub micron (nano-particulate) particles arrangement are shown schematically in Fig. 1. Such porous structure is only useful if the pores are decorated with an electronic conductor – in our case with a thin carbon film resulting from citrate degradation.

In this contribution, we summarize briefly our work on $LiFePO_4$ and compare it with the new results on $LiMnPO_4$. We show that the same synthetic route could be applied generally to any $LiMPO_4$-based cathode material (M = Fe and/or Mn).

2. Experimental

The samples were prepared using a standard sol–gel method [15]. As a starting precursor, iron (III) citrate (Aldrich, 22,897-4) or one part of manganese (II) acetate tetrahydrate ($C_4H_6O_4Mn{\cdot}4H_2O$, Fluka, 63537) and two parts of citric acid ($C_6H_8O_7{\cdot}H_2O$, Kemika, 0319506) were dissolved at 60 °C in water. Separately, an equimolar water solution of LiH_2PO_4 was prepared from lithium phosphate (Li_3PO_4, Aldrich 33,889-3) and phosphoric (V) acid (H_3PO_4, Aldrich 31,027-1). Clear solutions were mixed together and dried at 60 °C for 24 h. After thorough grinding with a mortar and pestle, the obtained xerogel was fired in an inert (pure argon) atmosphere at 700 °C ($LiFePO_4$ and $LiMn_{0.6}Fe_{0.4}PO_4$), or 900 °C ($LiMnPO_4$) for 10 h.

Electrodes were prepared by casting and pressing a mixture of 85 wt.% of the as-synthesized material, 7 wt.% of a PTFE binder (Aldrich 44,509/6) and 8 wt.% of carbon black (Printex XE2, Degussa) on aluminium foil followed by drying in vacuum at 120 °C for 24 h. The active material loading was about 5 mg cm^2 and the typical thickness of the active layer was 50 μm. The electrolyte used was a 1 M solution of $LiPF_6$ in EC:DMC (1:1 ratio by volume), as received from Merck.

A laboratory-made three-electrode test cell was used to carry out the electrochemical tests. The working and the counter (lithium) electrodes were held apart with two separators (Celgard No. 2402) between which a thin strip of lithium serving as a reference electrode was positioned. The cells were assembled in an argon-filled glove box at room temperature. Charge–discharge curves were recorded using an EG&G 283 Potentiostat/Galvanostat at room temperature. The constant current during cell cycling was set to a value between 8.5 and 0.85 A g^{-1} (corresponding roughly to *C*/20 and 5*C*, respectively). The geometric surface area of the working electrode was always 0.5 cm^2. The *C*-rate performance determination was always based on the mass of olivine phase only (the amount of carbon obtained from citrate anion degradation was substracted).

Characterisation techniques such as X-ray powder diffraction (XRD), ^{57}Mössbauer spectroscopy and thermogravimetric analysis are described elsewhere [14,16].

The textural properties were studied in the macroporous range by transmission electron microscopy (TEM) equipped with electron diffraction (Phillips EM 301) and scanning electron microscopy (Supra 35LV). The properties of porous composite in the 4–200 nm range were determined by nitrogen adsorption at 77 K using an ASAP 2000 instrument from Micromeritics. A sample of mass around 200 mg was loosely pressed into a wafer, then evacuated at 573 K under 0.1 Pa prior adsorption.

3. Results and discussion

Citrate anion is a suitable precursor for preparation of transparent gels with lithium, phosphate, citrate and transition metal (e.g. Fe, Mn, ...) ions. The obtained xerogels are homogenous on the molecular level and after thermal decomposition micro-sized $LiMPO_4$/C composite particles are obtained. In our previous reports [14,16] we have shown that the citrate anion affects the properties of the resulting $LiFePO_4$/C composites in two directions that crucially determine their electrochemical performance: (a) due to development of gases during degradation of citrate anion the resulting $LiFePO_4$ particles are significantly porous and (b) the remaining solid products of citrate degradation (basically pure car-

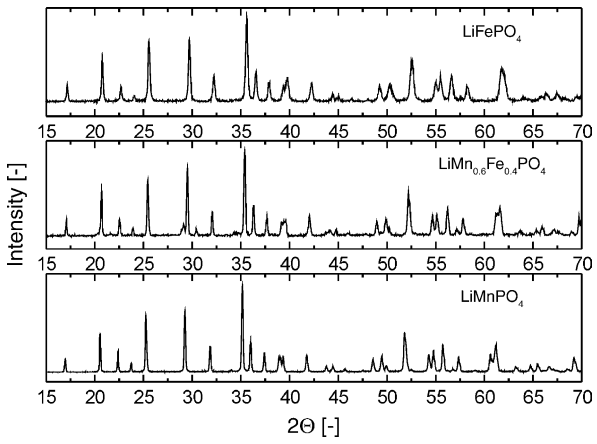

Fig. 2. X-ray diffraction patterns of $LiFePO_4$/C, $LiMn_{0.6}Fe_{0.4}PO_4$/C and $LiMnPO_4$/C composites.

bon) are deposited on all surfaces of the porous $LiFePO_4$ particles. After being filled with liquid electrolyte, the pores take care for fast ionic conduction while the deposited carbon serves as an electronic conductor. Additionally, the citrate ion (or its products) takes care for efficient reduction of Fe^{III} cations (using Mössbauer analysis, 98 at.% have been shown to be successfully reduced into Fe^{II} [16]). Prepared $LiMPO_4$/C composites ($LiFePO_4$/C, $LiMn_{0.6}Fe_{0.4}PO_4$/C and $LiMnPO_4$/C) were phase-pure according to their X-ray diffraction patterns (Fig. 2). In the case of thermal degradation in inert atmosphere, the content of carbon in as-synthesised $LiMPO_4$/C composite is about 3.2 wt.% [16] as determined using TGA analysis (it corresponds to mass difference between 380 and 480 °C).

The porous nature of $LiMPO_4$ materials has been studied qualitatively using SEM and TEM micrography and, also, quantitatively based on N_2 adsorption isotherms. At low magnification, SEM micrographs reveal a rough skeleton of $LiFePO_4$/C composite where most of the composite resembles a fragile "chess-like" structure (Fig. 3a). A closer view of the rough surface shows numerous apertures in the sub-micron range Fig. 3c. However, these small apertures lead into much larger voids inside the particle, as seen in the cracked crystallites shown in Fig. 3c ($LiFePO_4$/C composite) and Fig. 3d ($LiMnPO_4$/C composite). Detailed comparison of Fig. 3c and d shows no significant difference in textural properties of both $LiMPO_4$/C composites studied (that is, M = Mn and Fe).

A higher magnification also reveals the presence of much smaller apertures (of the order of 10 nm) (Fig. 4a) on the surface that, immediately below the surface, are continued into an interlaced system of mesopores/macropores (Fig. 4b). This qualitative picture of pores and voids of different dimensions has been confirmed with a quantitative analysis. Namely measurements of N_2 adsorption isotherms show a large hysteresis, which belongs to type IV with a flat type H3 hysteresis loop lacking of a clear plateau at saturation range. This result suggests that pores are distributed continuously in the meso and macro porous ranges [14]. Detailed analysis shows that average pore size is 60–90 nm (Fig. 5), thus in the meso-

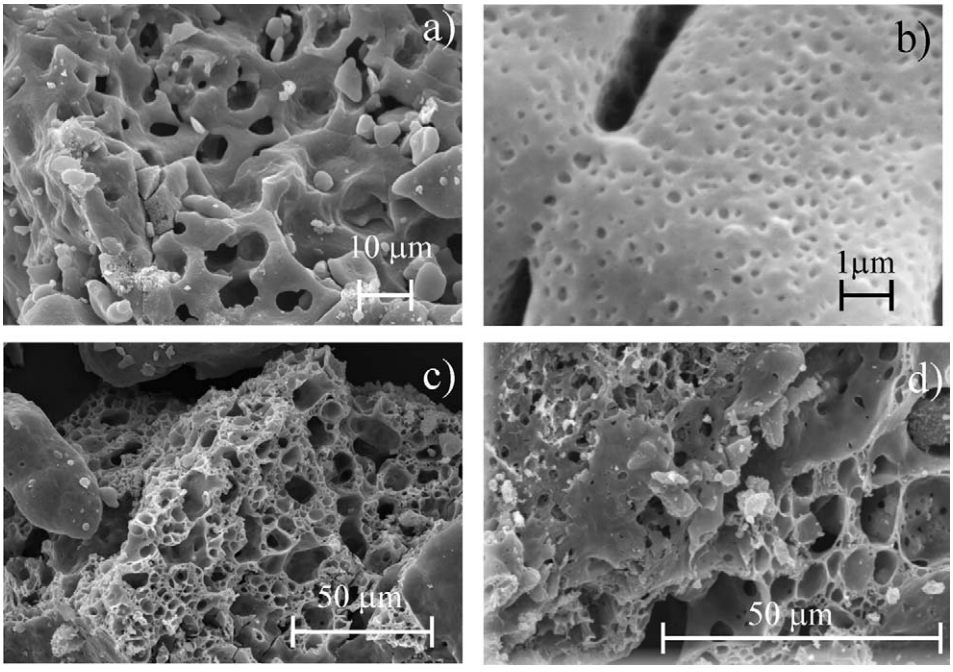

Fig. 3. SEM micrographs of various samples: (a) fragile "chess-like" structure of $LiFePO_4$/C composite, (b) rough surface of porous $LiFePO_4$/C composite with apertures, (c) particle interior with large voids and interlaced pore system in $LiFePO_4$/C composite and (d) particle interior with large voids and interlaced pore system in $LiMnPO_4$/C composite.

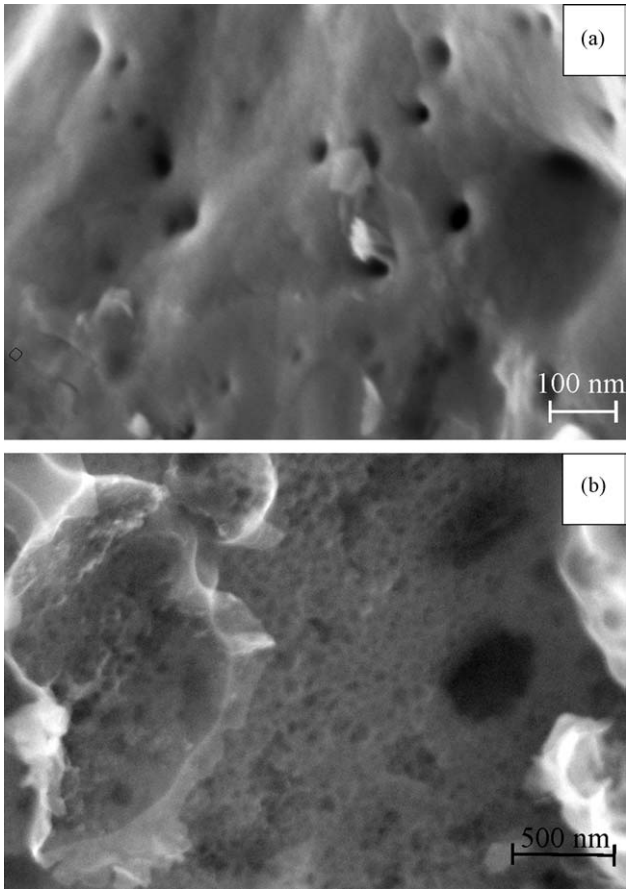

Fig. 4. SEM micrographs at higher magnification revealing that apertures (a) and pores (b) are mainly in mesoporous range.

porous range, and the surface area is about 20–25 $m^2 g^{-1}$. The above-mentioned textural properties are highly dependent on the type of synthesis (the present numbers refer to sol–gel samples), as well as on the heating rate during thermal combustion, xerogel aging, sol–gel concentration, etc. It is worth mentioning that the $LiMPO_4$/C samples contain

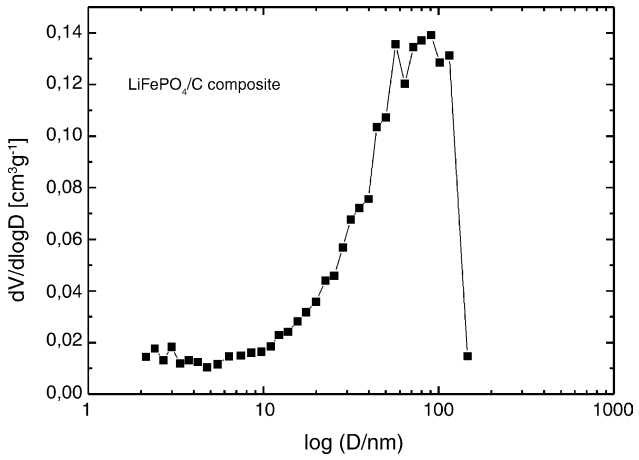

Fig. 5. Pore-size distribution for $LiFePO_4$/C composite prepared by sol-gel technique.

also pores in the microporous range (below 2 nm). These pores, however, pertain exclusively to the carbon phase (after burning off the carbon no microporosity was found, samples with higher carbon content show larger microporous volume, etc.). Another peculiarity of the porous $LiFePO_4$ materials prepared according to the citrate-based sol–gel is that their electron diffraction patterns reveal the presence of a single-crystalline $LiFePO_4$ phase. The electron diffraction pattern of a part (500 nm × 500 nm) of the porous particle in Fig. 6a is shown in b. This finding is not in contradiction with the XRD pattern (Fig. 2) showing polycrystalline nature of the sample as a whole. Analysis of the pattern in Fig. 6b reveals the [1 1 1] zone axis of the orthorhombic lattice of $LiFePO_4$ (Pattern 83-2092, CSD collection code: 200155). The $\{1\,1\,0\}$ spots, which are forbidden in bulk $LiFePO_4$ crystal by $h = 2n$ condition for $(h\,k\,0)$ reflections for the *Pnma* (62) space group, are apparently strong. Their appearance is explained by thin-foiled effect. The amplitude of diffracted beam is determined by shape factor, i.e. by structure factor for the whole volume, which contributes to the amplitude. If the volume in real space is small, the points in reciprocal space are replaced by rods. Ewald sphere cuts the rods running in parallel with the electron beam and the $\{1\,1\,0\}$ peaks appear in a porous material although they are prohibited in bulk compound. Their occurence is not in contradiction with the single-crystallinity of the the porous $LiFePO_4$ because only narrow masive parts of the sponge contribute to the coherent interference, while inputs from different pieces are only overlapped.

On the thin particles edges, the 1–2 nm thick carbon film was detected using a high-resolution tunnelling electron microscopy (HREM) (Fig. 6c). We believe that this carbon layer is responsible for good electronic conductivity of the composite material (average conductivity: 5×10^{-4} S cm^{-1}). Such a conductivity in combination with fast conduction of lithium ions along numerous pores results in the excellent electrochemical performance as displayed in Fig. 7. The reversible capacity of $LiFePO_4$/C (160 mAh g^{-1}, solid line) is close to the theoretical value and comparable to the best results for $LiFePO_4$ shown in literature. The performance of $LiMnPO_4$/C (ca. 40 mAh g^{-1} at *C*/20 rate, dotted line) is comparable to the scarce data available in literature [6,7]. As expected, a mixture of both transition elements gives a "mixed" curve involving both the redox potential of Fe^{II}/Fe^{III} and that of Mn^{II}/Mn^{III} (dashed curve). Using a composition of $LiMn_{0.6}Fe_{0.4}PO_4$/C we obtained a capacity of about 120 mAh g^{-1} at *C*/20.

The electrochemical rate performance and cycleability of $LiFePO_4$ are shown in Figs. 8 and 9. The reversible capacity with moderate current densities is close to 150 mAh g^{-1} (at *C*/5 and *C*/2 rate). Although at higher rates the reversible capacity starts to decrease, it is still close to 120 mAh g^{-1} at 5*C* (0.85 A g^{-1}) and is comparable to the one obtained with nanoparticulate composites. Note that the reversible capacity at a given current density was obtained by first discharging with a current density of 34 mA g^{-1} (*C*/5) up to 4.1 V versus lithium reference and then with additional discharging

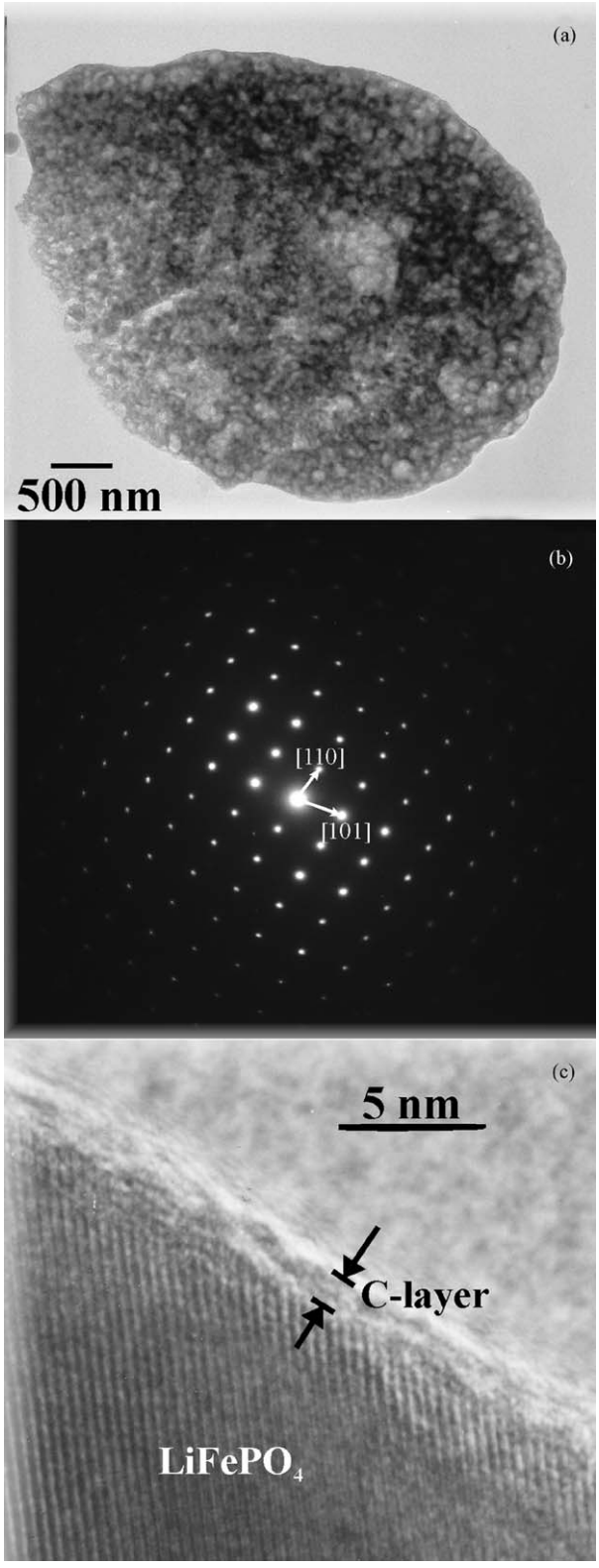

Fig. 6. (a) TEM micrograph of small particle of $LiFePO_4$/C composite, which reveals porosity in mesoporous and macroporous range, (b) electron diffraction pattern of the particle in Fig. 3a revealing the [1 $\bar{1}$ 1] zone of $LiFePO_4$ and (c) HRTEM of thin particle edge revealing [2 0 0] crystal planes of $LiFePO_4$ painted with a 1–2 nm thick layer of amorphous carbon.

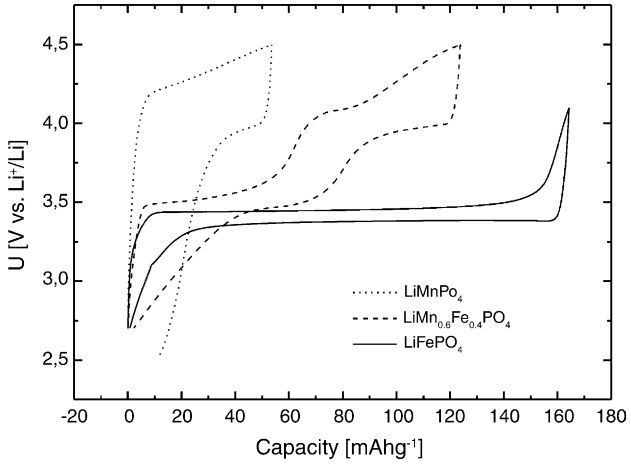

Fig. 7. Discharge/charge characteristics of porous $LiMPO_4$/C composites in the second cycle at current density 8.5 mA g^{-1} (*C*/20) at room temperature. Dotted line was obtained with a $LiMnPO_4$/C composite, dashed line with a $LiMn_{0.6}Fe_{0.4}PO_4$/C composite and solid line with a $LiFePO_4$/C composite.

with a current density of 8.5 mA g^{-1} (*C*/20) to the 4.1 V versus lithium reference, while charging was performed with the current densities as indicated in Fig. 8. From Fig. 9 we can see that the stability of the material is excellent (capacity fading is in order of a hundredth percent per cycle). The reversible capacity improvement in the first 20 cycles is, probably, either due to very slow penetration of electrolyte into particles' interior and/or due to formation of cracks in the amorphous carbon layer—both phenomena result in a higher active surface area for the electrochemical reaction. For a better performance of $LiMnPO_4$, even smaller distance between the pores is probably needed. At present, it is not clear whether electronic or ionic conductivity of the

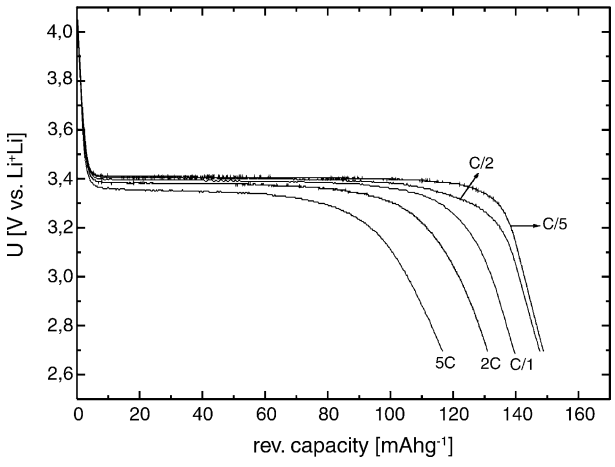

Fig. 8. Voltage profile of discharging curves for the porous $LiFePO_4$/C composite as a function of different current densities (*C*-rates). At a given rate, the cell was first charged with current density of 34 mA g^{-1} (*C*/5) to 4.1 V vs. lithium reference and then additionally charged with the current density 8.5 mA g^{-1} (*C*/20) to 4.1 V vs. lithium reference, before it was discharged to 2.7 V with the given current density (from 34 mA g^{-1} to 0.85 A g^{-1}, corresponding to *C*/5 to 5*C* rates).

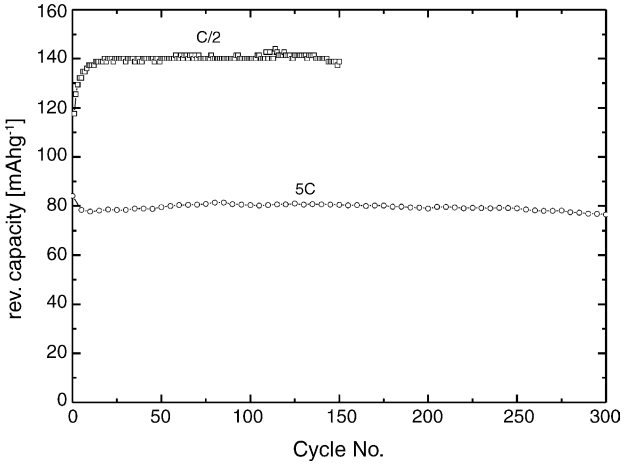

Fig. 9. Reversible capacity during continuous cycling at *C*/2 and 5*C* rates (the cell was discharged and charged with the same current density).

$LiMnPO_4$/C composite is the rate-determining step for overall kinetics.

In many experiments aimed to optimization of $LiMPO_4$/C electrochemical characteristics we have found that the composite particles should contain a high surface density of apertures, a considerable amount of interlaced mesopores corresponding to a surface area of at least $25\,m^2\,g^{-1}$ and an appropriate amount of carbon (about 3 wt.% which is equivalent to a ca. 1–2 nm thick carbon surface film). Interestingly, the presence of smaller mesopores with no apertures on the rough surface such as obtained using a solid-state synthesis instead of sol–gel method does not lead to a further improvement [14]. All these data confirm our previous picture showing the relation between the morphology and the electrochemical performance of the composite material. Surface apertures and internal pores are essential for fast delivery of ions to the spots of electrochemical reaction. It seems that mesopores serve optimally for this purpose. Although the primary role of carbon film is delivery of electrons to the place of electrochemical reaction, it must be thin enough or even porous to allow easy penetration of lithium ions perpendicularly to the film. Furthermore, thin carbon film (small amount of total carbon) prevent excessive occurrence of inactive Fe^{III} phases.

To summarize this part of discussion, we might say that the above strategy to prepare porous, carbon decorated $LiMPO_4$ composite material leads to similar electrode performance as the strategy of preparing sub-micron carbon-coated $LiMPO_4$ particles or particles embedded in a carbon matrix. The proposed synthesis is easy, it involves only one heating step and is free of health and environment hazards recently associated with nanoparticulate nature of materials [17,18].

4. Conclusions

By appropriate synthesis parameters and using appropriate precursors, it is possible to prepare porous, carbon-decorated $LiMPO_4$/C (M = Fe and/or Mn) composites with excellent electrochemical characteristics. The obtained structure could be described as an inverse picture of nanoparticulate arrangement, where pores serve as channels for lithium supply and the distance between the pores determines the materials kinetics. The porous architecture is achieved during the degradation of citrate anion and decomposition products form a thin layer of amorphous carbon on the walls of pores. Detailed analysis of $LiFePO_4$/C composite indicates that the average distance between the pores estimated from SEM and TEM micrographs is in the range of 30–60 nm, thus providing relatively short solid-state diffusion distances. On the other hand, the average diameter of pores is 60–90 nm, which is wide enough for unhindered lithium supply to the place of electrochemical reaction. The optimal carbon content needed for sufficient electron conductivity but, also, good ion permeability, is in the range of 3 wt.% (corresponding to 1–2 nm thickness of surface carbon layer). As expected, within the samples of $LiMPO_4$/C with comparable microstructures, $LiFePO_4$/C shows the best results, followed by mixed Fe, Mn olivines while pure $LiMnPO_4$/C shows the poorest performance (ca. $40\,mAh\,g^{-1}$ at *C*/20).

Acknowledgement

The financial support from the Ministry of Education, Science and Sport of Slovenia is fully acknowledged.

References

[1] A.K. Padhi, K.S. Nanjundaswamy, J.B. Goodenough, J. Electrochem. Soc. 144 (1997) 1188–1194.
[2] N. Ravet, J.B. Goodenough, S. Besner, M. Simoneau, P. Hovington, M. Armand, Proceedings of the 196th ECS Meeting, Hawaii, October, 1999, pp. 17–22.
[3] H. Huang, S.-C. Yin, L.F. Nazar, Electrochem. Solid-State Lett. 4 (2001) A170–A172.
[4] A. Yamada, S.-C. Chung, J. Electrochem. Soc. 148 (2001) A960–A967.
[5] G. Li, H. Azuma, M. Tohda, Electrochem. Solid-State Lett. 5 (2002) A135–A137.
[6] C. Delacourt, P. Poizot, M. Morcrette, J.-M. Tarascon, C. Masquelier, Chem. Mater 16 (2004) 93–99.
[7] M. Yonemura, A. Yamada, Y. Takei, N. Sonoyama, R. Kanno, J. Electrochem. Soc. 151 (2004) A1352–A1356.
[8] D. Arcon, A. Zorko, P. Cevc, R. Dominko, M. Bele, J. Jamnik, Z. Jaglicic, I. Golosovsky, J. Phys. Chem. Solids 65 (2004) 1773–1777.
[9] D. Arcon, A. Zorko, R. Dominko, Z. Jaglicic, J. Phys.: Condens. Matter 16 (2004) 5531–5548.
[10] S. Franger, F. Le Cras, C. Burbon, H. Rouault, Electrochem. Solid-State Lett. 5 (2002) A231–A233.
[11] A. Singhal, G. Skandan, G. Amatucci, F. Badway, N. Ye, A. Manthiram, H. Ye, J.J. Xu, J. Power Sources 129 (2004) 38–44.
[12] S. Panero, B. Scrosati, M. Wachtler, F. Croce, J. Power Sources 129 (2004) 90–95.
[13] S.Y. Chung, J.T. Blocking, Y.M. Chiang, Nat. Mater. 2 (2002) 123–128.

[14] R. Dominko, J.M. Goupil, M. Bele, M. Gaberscek, M. Remskar, D. Hanzel, J. Jamnik, J. Electrochem. Soc. 152 (2005) A858–A863.
[15] M. Bele, R. Dominko, M. Gaberscek, J. Jamnik, Pat. Appl. P-200300135, Slovenia (2003).
[16] R. Dominko, M. Bele, M. Gaberscek, M. Remskar, D. Hanzel, S. Pejovnik, J. Jamnik, J. Electrochem. Soc. 152 (2005) A607–A610.
[17] R.F. Service, Science 300 (2003) 243.
[18] G. Brumfiel, Nature 424 (2003) 246–248.